Cancer Therapy: Clinical

Clinical Cancer Research

Antibiotic Treatment Decreases Microbial Burden Associated with Pseudomyxoma Peritonei and Affects β-Catenin Distribution

Cristina Semino-Mora[1], Traci L. Testerman[4], Hui Liu[1], Jeannette M. Whitmire[1], Kimberley Studeman[2], Yali Jia[4], Thomas J. McAvoy[3], Jennifer Francis[4], Carol Nieroda[4], Armando Sardi[4], D. Scott Merrell[1], and Andre Dubois[1]

Abstract

Purpose: Pseudomyxoma peritonei is an understudied cancer in which an appendiceal neoplasm invades the peritoneum and forms tumor foci on abdominal organs. Previous studies have shown that bacteria reside within pseudomyxoma peritonei tumors and mucin. Thus, we sought to analyze the effect of antibiotics on bacterial density and β-catenin expression within pseudomyxoma peritonei samples.

Experimental Design: The study included 48 patients: 19 with disseminated peritoneal adenomucinosis (DPAM) and 29 with peritoneal mucinous carcinomatosis (PMCA). Fourteen patients were given antibiotics (30 mg lansoprazole, 1 g amoxicillin, and 500 mg clarithromycin) twice a day for 14 days. One week after completion of therapy, surgery was conducted and specimens were harvested for pathology, bacterial culture, ISH, and immunohistochemistry.

Results: ISH showed the presence of bacteria in 83% of the patient samples, with a higher *Helicobacter pylori* density observed in PMCA versus DPAM. PMCA patients treated with antibiotics had a significantly lower bacterial density and decreased β-catenin levels in the cytoplasm, the cell nuclei, and mucin-associated cells. Although not significant, similar trends were observed in DPAM patients. Cell membrane β-catenin was significantly increased in both DPAM and PMCA patients receiving antibiotics.

Conclusions: Bacteria play an important role in pseudomyxoma peritonei. Antibiotic treatment improved the histopathology of tissue, particularly in PMCA patients. In PMCA, antibiotics decreased bacterial density and were associated with a significant β-catenin decrease in the cytoplasm, cell nuclei, and mucin along with a small membrane increase. These results suggest that antibiotics offer potential protection against cell detachment, cellular invasion, and metastasis. *Clin Cancer Res; 19(14); 3966–76.* ©*2013 AACR.*

Introduction

Pseudomyxoma peritonei is characterized by the presence of multifocal peritoneal and omental implants of mucus-secreting epithelial cells and dissecting gelatinous ascites (1). This complex disease is found in 0.02% of laparotomies, and its incidence is threefold higher in females than in males (2, 3). Pseudomyxoma peritonei usually originates from a perforated low-grade appendiceal mucinous neoplasm or appendiceal adenocarcinoma that protrudes into the peritoneum, and the initial presentation of the disease often includes increased abdominal girth and/or appendicitis-like symptoms (4). Pseudomyxoma peritonei can take on a protracted course if the histopathology is that of disseminated peritoneal adenomucinosis (DPAM), or rapidly evolve as a highly malignant tumor with peritoneal mucinous carcinomatosis (PMCA) histopathology. Current treatment combines cytoreductive surgery (resection of the tumor and peritoneal implants) and intraperitoneal hyperthermic chemotherapy (5–8). Despite extensive resections, pseudomyxoma peritonei frequently relapses and 5-year survival is only 53% (9), although survival is significantly better if lymph nodes are negative (5-year survival is 76% for lymph node-negative patients and 11% for lymph node-positive patients; $P < 0.001$; ref. 10). Even in patients with low-grade appendiceal mucinous neoplasms, most patients succumb to the disease due

Authors' Affiliations: [1]Uniformed Services University and United States Military Cancer Institute, Bethesda; [2]Mercy Medical Center, Baltimore; [3]University of Maryland, College Park, Maryland; and [4]Louisiana State University Health Sciences Center-Shreveport, Shreveport, Louisiana

Note: Supplementary data for this article are available at Clinical Cancer Research Online (http://clincancerres.aacrjournals.org/).

Corresponding Authors: Thomas J. McAvoy, University of Maryland, College Park, MD 20742. Phone: 301-405-1935; Fax: 301-314-9126; E-mail: mcavoy@umd.edu; and D. Scott Merrell, Department of Microbiology, Uniformed Services University of the Health Sciences, Room B4140, Bethesda, MD 20814. Phone: 301-295-1584; Fax: 301-295-3773; E-mail: douglas.merrell@usuhs.edu

doi: 10.1158/1078-0432.CCR-13-0616

©2013 American Association for Cancer Research.

Translational Relevance

Pseudomyxoma peritonei is an underresearched abdominal cancer that originates from an appendiceal neoplasm. Patients frequently relapse and succumb to the disease, necessitating the development of novel therapeutics to treat patients. Recent studies have indicated the presence of bacteria within the tumors and mucin of pseudomyxoma peritonei patients. The study herein indicates that antibiotic treatment significantly reduces bacterial density along with β-catenin levels in the cytoplasm, the cell nuclei, and mucin-associated cells of peritoneal mucinous carcinomatosis (PMCA) patients. In addition, the β-catenin levels within membranes significantly increase in both disseminated peritoneal adenomucinosis and PMCA patients. The renormalization of β-catenin distribution combined with the reduction in bacterial density make antibiotic treatment a potential therapeutic for pseudomyxoma peritonei disease.

to recurrent mucoid ascites, proliferation of gelatinous mucin, and mechanical compression and obstruction of abdominal organs, heart, and lungs (11).

A key aspect of colon cancer and several other cancers is deregulation of the Wnt/β-catenin pathway (12). The transmembrane protein β-catenin is associated with the cytoplasmic region of E-cadherin within adherens junctions. In normal, polarized gut epithelial cells, β-catenin provides a linkage mechanism between cytoskeletal proteins and cell-to-cell junctional proteins (e.g., E-cadherin), allowing cells to tightly bind to each other (13). These interactions are crucial for maintenance of epithelial cell polarity, regulation of cell growth, and cell-to-cell focal adhesion. During carcinogenesis, β-catenin relocates into the cytoplasm and nucleus. Loss of membrane β-catenin leads to cell separation and migration, movement of abnormal neoplastic cells to the stroma, entry into blood vessels, and metastatic spread to different tissues through the bloodstream (14). Furthermore, following nuclear translocation, β-catenin interacts with T-cell factors (TCF) or lymphocyte-enhancer factors that can then act as transcription factors. Thus, β-catenin nuclear localization triggers expression of various genes, including genes required for cell proliferation (15).

Several infectious agents have been found to stimulate cell proliferation via the Wnt/β-catenin pathway. In fact, the potential for certain viruses to cause cancer has been recognized for some time. Recent studies suggest that Epstein–Barr virus, Kaposi's sarcoma-associated virus, and hepatitis C virus promote carcinogenesis by activating the Wnt/β-catenin pathway (16, 17). Some bacteria also influence the Wnt/β-catenin pathway. *Helicobacter pylori* expresses numerous virulence factors that promote carcinogenesis, including the cytotoxin-associated gene A (CagA). Translocation of CagA into epithelial cells results in changes in expression of β-catenin (18) as well as causes nuclear accumulation of β-catenin (19), which is associated with aggressive and invasive tumors (20). *Salmonella* and *Chlamydia trachomatis* also stimulate epithelial proliferation via the Wnt/β-catenin pathway (21, 22).

Although pseudomyxoma peritonei patients have no symptoms of peritonitis, we previously hypothesized that intestinal bacteria spread to the peritoneum at the time of appendiceal perforation. In keeping with this idea, we recently showed that *H. pylori* and other bacteria can be detected in pseudomyxoma peritonei tissues (23). Given this finding, herein we studied the effect of preoperative antibiotic therapy on bacterial density, and on the concurrent expression of β-catenin within the neoplastic cancerous cells of DPAM and PMCA patients. We observed that after antibiotic treatment, PMCA patients showed a significant decrease in bacterial density along with significantly decreased β-catenin expression in the cytoplasm, nuclei, and mucin. We found that in neoplastic cancerous cells, β-catenin is redistributed into the cytoplasm and accumulates in different areas of the cytosol and ground substance (connective tissue in the stroma that supports fibers). *En masse*, our data suggest that antibiotic treatment of PMCA may affect the carcinogen pathway elicited by β-catenin and may serve as a novel treatment of this understudied cancer.

Materials and Methods

Patients, histopathology, and treatment

Forty-eight patients with the diagnosis of peritoneal dissemination of appendiceal mucinous neoplasms that had been scheduled to undergo laparotomy for staging, extensive cytoreductive surgery, and hyperthermic intraperitoneal chemotherapy were studied. Patients' age was 53 ± 2 years and weight 73 ± 2 kg (means and SEM).

Observation and analysis of biopsies stained with hematoxylin and eosin (H&E) from cytoreductive surgical specimens by a board certified and experienced pathologist allowed tumor classification as either DPAM or as the more malignant PMCA (24). Tissue from a patient with a nonperforated, nonneoplastic appendix (NNA) was used as a control. Analysis of the grade of inflammation was conducted according to conditions previously described (25).

Three weeks before surgery, an open label anti-*H. pylori* triple therapy (Prevpac, i.e., 30 mg lansoprazole, 1,000 mg amoxicillin, and 500 mg clarithromycin given twice a day for 14 days) was given to a total of 14 of the pseudomyxoma peritonei patients: 6 DPAM and 8 PMCA. A total of 34 patients received no antibiotics and were maintained as untreated controls: 13 DPAM and 21 PMCA. One week after completion of the antibiotic therapy, patients and controls underwent cytoreductive surgery (resection of the tumor and peritoneal implants) and hyperthermic intraperitoneal chemotherapy to achieve complete or near-complete resection of pseudomyxoma peritonei cancerous tissues (8).

ISH studies

Probes. Two previously described *16S rDNA* bacterial probes (23) labeled with biotin were as follows: (i) a probe

that can detect 19,973 typed and nonculturable bacteria (TNCB; including *Campylobacter jejuni*, *Escherichia coli*, *Salmonella enterica*, *H. pylori*, and *Enterococcus faecalis*; 5′-AGCAAA CAG GAT TAG ATA CCC TGG TAG TCC AC-3′); and (ii) a probe specific for *H. pylori* (5′-ATT TCA CAC CTG ACT GAC TAT CCC GCC TAC GCG-3′; ref. 26). In initial experiments, we used both cRNA and cDNA probes concurrently, and confirmed earlier observations that these 2 probes can detect the same bacteria (27).

Paraffin blocks of formalin-fixed tissue were sectioned (5 μm) and analyzed as previously described (27). Briefly, each unstained section was deparaffinized, prehybridized, hybridized with denatured probe solution, and then incubated for 18 hours with a probe labeled with biotin followed by the removal of unbound probe using saline citrate solution. DNA was detected by incubating the slide for 2 hours with streptavidin-conjugated alkaline phosphatase (Roche Diagnostic; 1:500 dilution in blocking immuno-Tris buffer), washing, and applying, the chromogenic substrate BCIP/NBT/kit (5-bromop-4-chloro-3-indolyl phosphate/nitro-blue-tetrazolium), yielding a blue color reaction (Vector Labs). The slide was then counterstained with Nuclear Fast Red, washed in water, dehydrated, cleared in xylene, air dried, and mounted with permount. TNCB and *H. pylori 16S rDNA* were detected in serial sections under bright light as follows: first section: detection of TNCB *16S rDNA*, second section: detection of *H. pylori 16S rDNA*. Parallel dual FISH studies (27) were also conducted using the *16S rDNA*-TNCB probe labeled with biotin and then detected with avidin labeled with fluorescein–fluorescein isothiocyanate (FITC; green reaction), and the *16S rDNA-H. pylori* probe labeled with digoxigenin and then detected with anti-digoxigenin mouse monoclonal antibody conjugated to biotin (Abcam) and then detected using avidin-Tx red (red reaction). Colocalization of both TNCB and *H. pylori* was visualized as yellow.

As previously described (27), control for nonspecific binding included: (i) sense probe instead of antisense probe, (ii) hybridization buffer instead of the antisense probe, (iii) unlabeled antisense probe, (iv) digoxigenin or biotin-labeled probe for a sequence completely unrelated to man and prokaryotes—the scorpion *Buthus martensi* Karsch neurotoxin sequence (5′-GGC CAC GCG TCG ACT AGT AC-3′; ref. 28), (v) RNase A pretreatment (Roche), (vi) DNase I pretreatment (Roche), and (vii) RNase + DNase I pretreatment.

For fluorescence, a Nikon Eclipse 80i microscope DS black-white camera with a DS-L2 control unit was used and software from NIS-Elements Advanced Research was used for analysis and reproduction of β-catenin images. For brightfield microscopy, an Eclipse 800 Nikon microscope with digital camera (QCapture Pro, Micropublisher 6.0; Burnaby) was used for analysis and reproduction of bacterial images (TNCB and *H. pylori*). Fluorescence immunohistochemistry (FIHC) was used for studies of β-catenin. Two different studies were conducted:

Laser confocal microscopy was used to quantify cell membrane and nuclear localization of β-catenin. Antigen retrieval was first achieved by sequentially treating deparaffinized sections with saline citrate solution in a pressure cooker system for 9 minutes (27). β-Catenin expression was analyzed using a mouse anti-β-catenin monoclonal antibody (Santa Cruz Biotechnology, Inc.) at 1:150 dilution followed by biotinylated anti-mouse immunoglobulin G and avidin, labeled with either FITC for β-catenin cell membrane localization or Texas red for β-catenin nuclear localization. For nuclear localization, DNA was also stained using 4′,6-diamino-2-phenylindole (DAPI) because it specifically binds DNA without overlap with fluorochromes. Importantly, DAPI binds DNA (heterochromatin and euchromatin) of an interphase nucleus. In contrast to usual dual-fluorescence stains, DAPI stain cannot be easily merged with the expression of any fluorochrome (in this case with β-catenin-Texas red) to produce a third color because nuclear DNA is bound to β-catenin (first layer of procedure) and, as a result, DAPI binding to DNA is not as efficient at the same site. However, DAPI can bind to DNA that is not bound to β-catenin.

β-Catenin compartment localization was determined from standard fluorescence (FIHC) of paraffin sections mounted with Vectashield alone (w/o DAPI) and observed using a Nikon Eclipse 80i microscope as described earlier. The following tissue types were analyzed: (i) epithelia; (ii) lymphocytes, monocytes, and granulocytes; (iii) stroma (connective tissue, vessels, fibroblasts, and fibers); and (iv) mucin pools. In addition, specific analyses of (i) lateral cell–cell contact and (ii) cytoplasm localization were conducted.

Fluorescence IHC images were observed and reproduced using the same microscope and digital camera described earlier for the ISH studies.

For β-catenin nuclear localization, sections were mounted using Vectashield containing DAPI and confocal images were collected on a Zeiss S710 NLO laser scanning confocal microscope (Carl Zeiss) equipped with a 63× oil immersion lens (1.4NA). DAPI-stained samples were excited with a 405-nm laser diode and emitted light in the 410 to 556 nm range was collected. For Texas red–stained samples, a laser line of 561 nm was used for excitation and light between 566 and 690 nm was used for imaging (BIC, USUHS). Phosphate buffer solution instead of the first β-catenin antibody was used as a negative control.

Morphometric analysis

Quantitation of bacteria and β-catenin. Determination of bacterial and β-catenin density in cellular compartments was conducted as previously described (27). Briefly, an intraocular grid-based method was used to examine samples by a microscopist who was blinded to the histopathologic diagnoses (i.e., DPAM or PMCA) as well as antibiotic treatment category. The number of bacterial clusters expressing *16S rDNA* of TNCB and/or *H. pylori* was quantified at 400× magnification in 3 randomly selected fields of view according to a modification of the point-counting stereological method, and using an intraocular reticle of 27-mm diameter, covering 3578 μm^2 (i.e., 17,892 μm^3 for 5-μm-thick sections; Kr409, Klarman Rulings, Inc.; ref. 23). Counting of the number of intersections of vertical and horizontal lines that overlapped a bacterium in the area

delimited by a projected grid on the tissue was conducted. All data were expressed as means ± SEM number of bacteria per 10^6 μm^3 (representing an imaginary cube with sides of 100 μm or 0.1 mm).

Total β-catenin density in biopsies was determined in a similar fashion and expressed as Vvi (volumetric density or volume occupied for the β-catenin reaction) in 10^6 μm^3 of tissue.

Computerized quantification of β-catenin in the nuclei. Nuclear localization of β-catenin and analysis were conducted using a Zeiss 710 NLO laser scanning confocal microscope (Carl Zeiss) as described earlier (BIC, USUHS).

Software developed by TM using a MATLAB platform and associated toolboxes (http://www.mathworks.com/) was used to quantify the fraction of the nucleus occupied by β-catenin in confocal microscopic pictures of IHC sections that had been double stained for both β-catenin (Texas red) and DNA (DAPI; Supplementary Methods). In brief, the percent of nuclei volume occupied by β-catenin was calculated as the number of bright red pixels that overlapped the dark blue DAPI stain divided by total nuclei pixels (nuclei in blue) multiplied by 100.

Statistical analysis

Statistical significance was determined using *t* tests to compare results in patients receiving antibiotics versus no antibiotics in each cell of the tables. Values were expressed as means ± SEM.

Results

Pathological evaluation of DPAM and PMCA

H&E-stained sections were examined to determine the histopathology of the pseudomyxoma peritonei samples. Sections from DPAM patients (Fig. 1A) showed the presence of abundant extracellular mucin (pale pink areas with blue streaks) surrounded by dark pink collagen bands. Mucin pools were surrounded by connective tissue septa supporting the mucin deposits. Strips of mucinous epithelial lining and scattered chronic inflammatory cells, including lymphocytes and macrophages, were also characteristics of DPAM (Fig. 1A, left). Low-grade adenomatous dysplasia was seen without evidence of mitosis, which is consistent with the more indolent nature of DPAM. Mesothelial hyperplasia, vascular congestion (engorged blood vessels), and chronic inflammation were present in the peritoneal lining adjacent to extracellular mucin in DPAM sections (Fig. 1A, right).

In PMCA patient sections (Fig. 1B–D), glands consisting of angulated gland-forming mucinous epithelium were frequent, often with destructive stromal invasion (Fig. 1B). High-grade cytologic atypia, mitotic activity (Fig. 1C), and

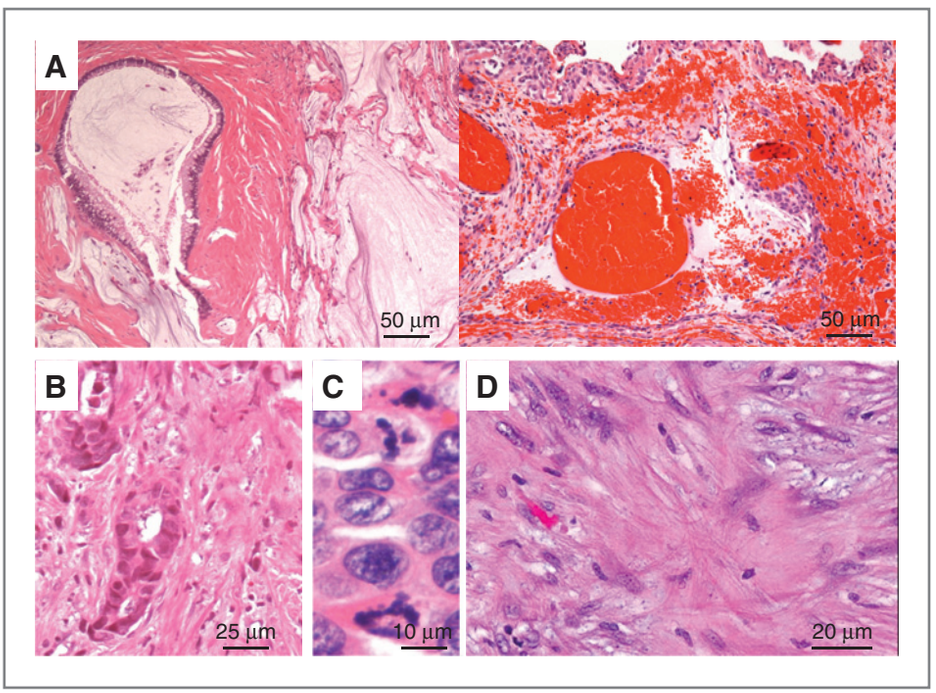

Figure 1. Pathologic examination of DPAM and PMCA tissue samples. Cytoreductive surgical specimens were collected, sectioned, stained with H&E, and evaluated to determine tumor classification, histopathology, and inflammation grade. DPAM samples (A) displayed extracellular mucin (pale pink areas with blue streaks) bordered by dark pink collagen bands supporting the mucin deposits. DPAM samples were further characterized by a mucinous epithelial lining, chronic inflammatory cells scattered throughout the tissue, and low-grade adenomatous dysplasia without mitosis (A, left). The peritoneal lining adjacent to the extracellular matrix in DPAM sections exhibited mesothelial hyperplasia, vascular congestion, and chronic inflammation (A, right). PMCA samples (B–D) presented with glands comprised of angulated gland-forming mucinous epithelium with destructive stromal invasion (B). In addition, the PMCA samples are distinctively identified from the DPAM sections based on the presence of high-grade cytologic atypia (C), mitotic activity (C), and inflammatory cells within desmoplastic stroma with fibrotic adhesions (D).

inflammatory cells within a desmoplastic stroma with fibrotic adhesions differentiate PMCA from DPAM (Fig. 1D); desmoplasia is a fibrotic reaction to malignant cells invading normal tissue. No significant differences in inflammatory cell densities were observed across the 2 disease types in H&E slides (scores of 0–3; ref. 29).

Presence of bacteria in DPAM and PMCA as determined by ISH

Our work has previously shown that *H. pylori* and other bacteria can be found in pseudomyxoma peritonei samples (23). We therefore sought to confirm these results using these independently obtained pseudomyxoma peritonei samples and ISH with probes that detect TNCB or *H. pylori*. Our initial qualitative analysis of samples from all 48 patients revealed that clusters of TNCB (Fig. 2A–C, left) and *H. pylori* (Fig. 2A–C, right) were present within 83% of the specimens: 76.9% of the untreated DPAM patients, 83.3% of the antibiotic-treated DPAM patients, 90.5% of the untreated PMCA patients, and 75% of the antibiotic-treated PMCA patients (Table 1). Both TNCB and *H. pylori* were present in mucinous epithelia and were associated with mucin-secreting and goblet cells, as well as pools of mucin. Figure 2B (left) shows TNCB bacteria within mucin deposits and in areas of abnormal neoplastic epithelia. *H. pylori* was similarly located in the mucin surrounded by abnormal neoplastic epithelia and goblet cells and attached to the cell membrane of neoplastic cells (Fig. 2B, right, and inset). TNCB and *H. pylori* were also observed in the connective tissue of the lamina propria (stroma; Fig. 2C, left and right, respectively), touching inflammatory cells located in the stroma, and surrounding epithelial cells in the intestinal glands.

To determine whether there was any effect of antibiotic treatment on the quantity of bacteria found per sample, individual bacteria were counted manually in 3 fields of view. As with the qualitative analysis, *H. pylori* and TNCB were detected in 83% of the patients. The 8 patients negative for both probes were as follows: 1 DPAM-A, 3 DPAM-noA, 2 PMCA-A, and 2 PMCA-noA, where "A" indicates antibiotic treatment and "noA" indicates no antibiotic treatment. On average, and as previously reported (23), *H. pylori* and TNCB densities were significantly higher in PMCA than in DPAM patients (*H. pylori*: 32.4 ± 5.2 vs. $13.0 \pm 3.2/10^6\ \mu m^3$, $P < 0.008$; TNCB: 63.3 ± 10.4 vs. $26.8 \pm 5.4/10^6\ \mu m^3$, $P < 0.01$). In addition, *H. pylori* and TNCB densities were significantly lower in PMCA patients who received preoperative antibiotics (*H. pylori* 12 ± 6 vs. $40 \pm 6/10^6\ \mu m^3$, $P < 0.01$ and TNCB 18.6 ± 7.4 vs. $80.4 \pm 12.2/10^6\ \mu m^3$, $P < 0.006$, respectively). However, there was no significant difference in bacterial density in DPAM patients after antibiotic treatment. Examples of the bacterial density with and without antibiotic treatment are illustrated in an area of pooled mucin using FISH staining (Fig. 3A–C; A: TNCB, B: *H. pylori*, C: merge). The TNCB probe binds to *H. pylori* as well as other species. Therefore, *H. pylori* overlaps TNCB and appears yellow when the images are merged, whereas non-*H. pylori* bacteria remain green in the merged image.

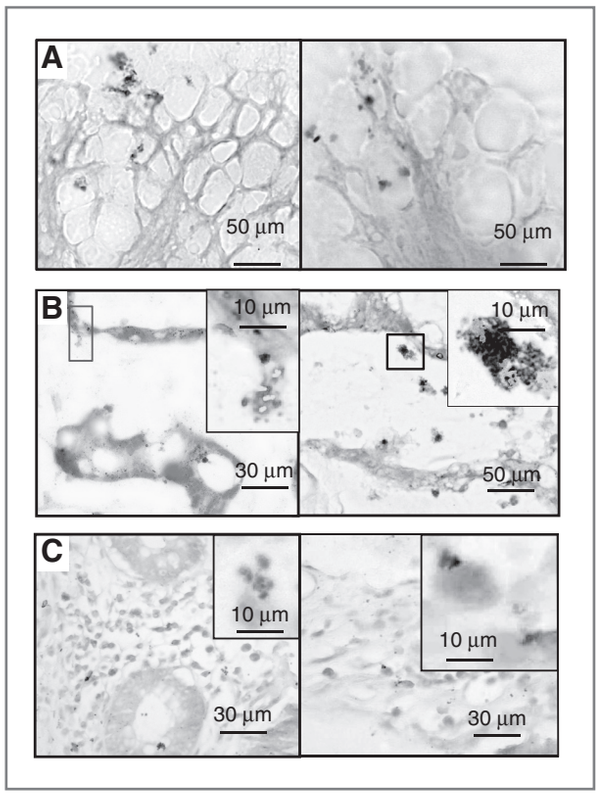

Figure 2. Identification of bacteria through ISH. Formalin-fixed tissue specimens from pseudomyxoma peritonei patients were serially sectioned and analyzed with (ISH) probes to detect all TNCB present (A, B, C, left) or specifically *H. pylori* (A, B, C, right). Clusters of TNCB (A, left) and *H. pylori* (A, right) were found in 83% of the analyzed tissue samples. TNCB (B, left) and *H. pylori* (B, right) were observed within the mucin encompassed by neoplastic epithelia and goblet cells. Both TNCB (C, left) and *H. pylori* (C, right) were also present in the connective tissue of the lamina propria (stroma), contacting inflammatory cells and epithelial cells in the intestinal glands.

Table 1. Bacterial distribution in pseudomyxoma peritonei samples

Group	% of samples containing bacteria	Relative number of *H. pylori*	Relative number of TNCB
DPAM	76.9	14.46	29.54
DPAM, antibiotic treated	83.3	9.90	21.0
PMCA	90.5	40.37	80.36
PMCA, antibiotic treated	75	11.54	18.54

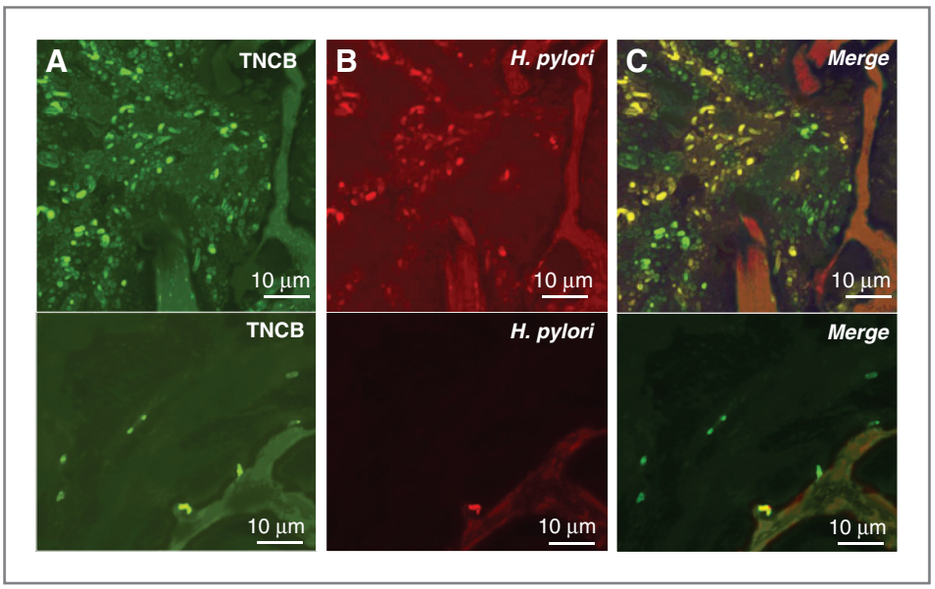

Figure 3. FISH analysis of bacterial density in mucin. Formalin-fixed tissue specimens from pseudomyxoma peritonei patients were serially sectioned and analyzed with FISH to identify all TNCB present (green; A) or specifically *H. pylori* (red; B) within a region of pooled mucin. In the merged images (C), the *H. pylori* staining converges with the TNCB staining to reveal a yellow color for *H. pylori* whereas all non-*H. pylori* bacteria appear green. A clear reduction in bacterial density is observed in a pseudomyxoma peritonei patient receiving antibiotic treatment (A–C, bottom) compared to an untreated pseudomyxoma peritonei patient (A–C, top).

The above results were obtained using probes that recognize 16S rDNA, which detects both live and dead bacteria. Because it was possible that some dead bacteria could still be detected, we evaluated *H. pylori* viability in a subset of PMCA patients using a 16S rRNA probe combined with polyclonal anti-*H. pylori* antiserum. As shown in Supplementary Fig. S1, virtually all of the *H. pylori* were alive in untreated PMCA patients, whereas very few remained viable in antibiotic-treated patients. These data suggest that the determined densities of bacteria are likely artificially high in patients that received antibiotic treatment.

β-Catenin in pseudomyxoma peritonei

Given that the Wnt pathway and β-catenin have been shown to be important in numerous forms of cancer, we investigated whether β-catenin quantities and localization were affected in pseudomyxoma peritonei and across pseudomyxoma peritonei types. We assessed this by initially quantifying total β-catenin in 5 random fields per sample from an NNA control and in the DPAM and PMCA sections. When all DPAM and PMCA cases were compared regardless of antibiotic treatment status, we observed that total β-catenin expression tended to be lower in DPAM than in PMCA ($1{,}721 \pm 297$ vs. $3{,}083 \pm 542$ Vvi/10^6 μm^3, $P < 0.062$; NS). When the antibiotic treatment state was taken into consideration across the disease states, antibiotics tended to decrease total β-catenin expression in PMCA patients ($P < 0.036$). However, expression was not significantly different in DPAM patients ($P < 0.36$; NS). Given that localization of β-catenin is crucial to its function inside the cell, we next examined localization within different cellular compartments qualitatively as well as quantitatively. Analysis of β-catenin staining within the NNA control indicated the presence of β-catenin in cell membranes and the lateral junctional complex (Fig. 4A and inset). In contrast, biopsies obtained from PMCA patients that did not receive antibiotics showed virtually no β-catenin staining at the intercellular boundary (Fig. 4B and inset); staining seems primarily cytoplasmic. However, as was noted with the total β-catenin assay, antibiotic treatment seemed to have some effect on β-catenin localization because a moderate to intense reaction was observed in the junctional complexes between some of the PMCA neoplastic cells after antibiotic treatment (Fig. 4C and inset). However, these values did not reach statistical significance when the junctional staining was quantitated for PMCA-A (451 ± 67 Vvi/10^6 μm^3) and compared to PMCA-noA (751 ± 207 Vvi/10^6 μm^3; $P < 0.36$). Antibiotics decreased β-catenin expression in the cytoplasm of PMCA patients who received treatment as compared to no antibiotics (739.9 ± 63.1 vs. 216.6 ± 41.5 Vvi/10^6 μm^3; $P < 0.0001$). When considered as a whole, β-catenin was increased in the stromal compartment of PMCA (A + noA; 1046.5 ± 193.4 Vvi/10^6 μm^3) as compared to DPAM (A + noA; 516.8 ± 70.1 Vvi/10^6 μm^3; $P = 0.0369$). This was especially true in the desmoplastic reactions of untreated PMCA patients (Fig. 4D). Finally, β-catenin levels found within the mucin, presumably due to the presence of infiltrating inflammatory cells, decreased in PMCA patients after antibiotic treatment (464.58 ± 139.418 Vvi/10^6 μm^3) as compared to no antibiotics ($2{,}179.70 \pm 303.38$ Vvi/10^6 μm^3; $P < 0.0021$). Conversely, DPAM did not show a significant difference in the mucin due to antibiotic treatment. As a result, there was a significant difference ($P < 0.005$) in the overall β-catenin staining of PMCA (A + NoA) mucin ($1{,}706.56 \pm 264.45$ Vvi/10^6 μm^3) as compared to DPAM (A + NoA) mucin (433.14 ± 104.55 Vvi/10^6 μm^3). Finally, although some change in β-catenin distribution was seen in the stromal region of PMCA patients, these changes were not significant.

Given that β-catenin is known to enter the nucleus and function as a transcription factor, and because our initial

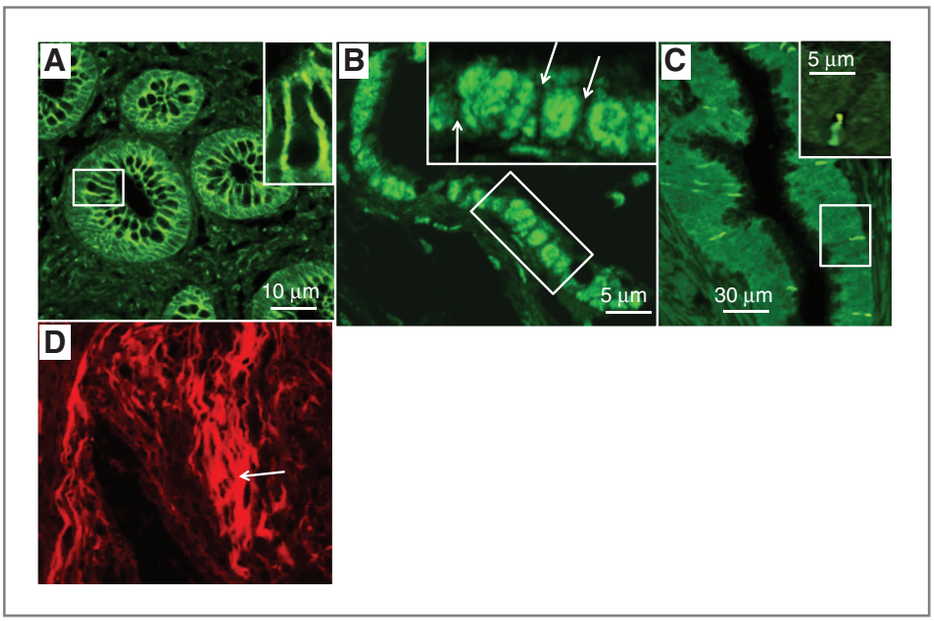

Figure 4. Qualitative assessment of β-catenin localization in pseudomyxoma peritonei samples. Formalin-fixed tissue samples from pseudomyxoma peritonei patients and an NNA control were sectioned and stained with an anti-β-catenin antibody. The NNA control (A) displayed strong staining at the boundaries between adjacent cells, showing the localization of β-catenin to cell membranes and the lateral junctional complex. Conversely, PMCA sections (B) exhibited primarily cytoplasmic staining of β-catenin and virtually no staining at the intercellular boundaries. Some staining was observed between PMCA neoplastic cells following antibiotic treatment (C). β-Catenin was very visible in the desmoplastic reactions within the stromal compartment of untreated PMCA patients (D).

staining did not allow us to discern which portion of the cytoplasmic β-catenin was actually in the nucleus, we used dual staining with DAPI and β-catenin along with a computerized quantification method to determine the fraction of the nucleus occupied by β-catenin. Control NNA tissue exhibited intense bright DAPI staining, but was negative for nuclear β-catenin (data not shown). Conversely, nuclear β-catenin was common in both PMCA and DPAM samples, as exemplified by the fluorescent staining of the nuclei shown in Fig. 5. In the high magnification insets, bright red color signifies β-catenin expression (A, arrow), whereas dark blue DAPI staining is seen when nuclear β-catenin is absent (B, arrowhead). When the images are merged (C), the intense red shows up without being affected by the blue DAPI stain. Of note, faint perinuclear β-catenin staining is seen around most DAPI-stained nuclei, indicating that β-catenin was present elsewhere in those cells. The percent of DAPI-stained nuclei occupied by β-catenin was not significantly different when all PMCA samples (A + NoA) were compared to DPAM samples (A + NoA) (20 ± 2.9 vs. $16.5 \pm 3.5\%$, $P < 0.451$; NS). However, administration of antibiotics resulted in a significant decrease in the percent of nuclear β-catenin present in PMCA (from $23.8 \pm 3.4\%$ to $11 \pm 4.4\%$, $P = 0.048$). Despite the fact that there was a strong trend toward decreased nuclear β-catenin, this significant difference was not seen with DPAM (from $18.9 \pm 4.8\%$ to $11.3 \pm 3\%$, $P < 0.152$; NS; Fig. 6A). As nuclear β-catenin dropped as a result of antibiotic treatment, the percentage of β-catenin located in the membrane as compared to the cytoplasm increased (Fig. 6B). This rise in membrane β-catenin was significant for both PMCA and DPAM patients.

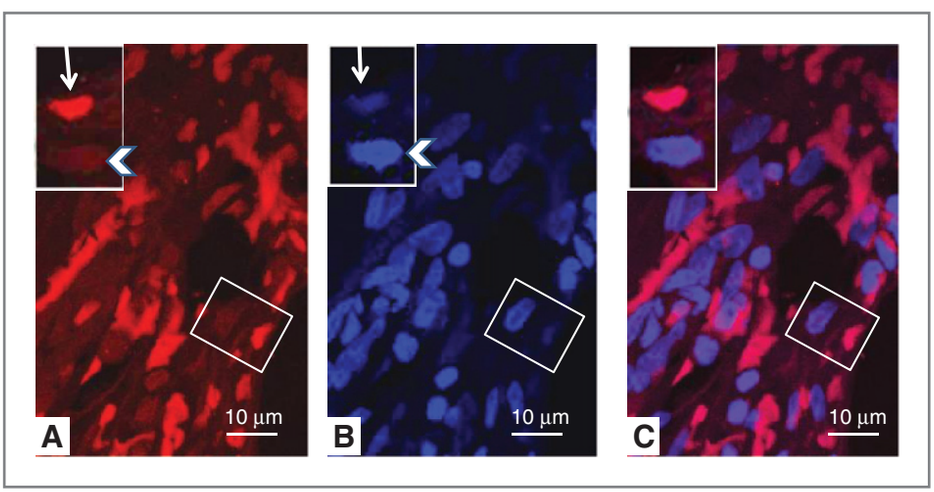

Figure 5. Immunofluorescence analysis of nuclear β-catenin. Formalin-fixed tissue samples from pseudomyxoma peritonei patients were sectioned and dual stained with an anti-β-catenin antibody and DAPI to observe the localization of nuclear β-catenin. As shown in A, bright red staining (arrow) indicates the presence of β-catenin, whereas B reveals the dark blue DAPI staining (arrowhead) appearing when β-catenin staining is absent. The merged image in C exhibits the intense red β-catenin staining unaffected by blue DAPI staining.

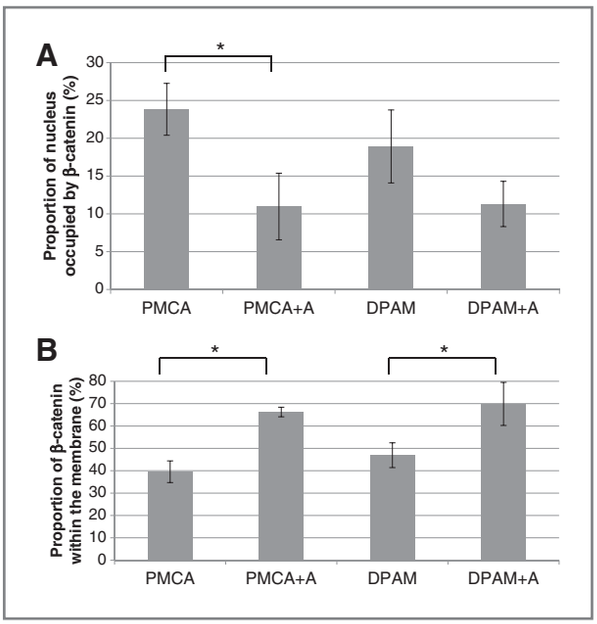

Figure 6. Quantitative evaluation of β-catenin localization. Formalin-fixed tissue samples from pseudomyxoma peritonei patients were sectioned and either stained solely with an anti-β-catenin antibody to determine membrane localization or stained with both an anti-β-catenin antibody and DAPI to determine the proportion of the nucleus occupied by β-catenin. Antibiotic treatment significantly reduced ($P = 0.048$) the proportion of the nucleus occupied by β-catenin (A) in PMCA patients. Though a reduction in nuclear β-catenin was observed in DPAM patients following antibiotic treatment as well, this change was not significant (A). The reduction in nuclear β-catenin was accompanied by a significant elevation in β-catenin within the membrane (B) for both PMCA ($P < 0.05$) and DPAM ($P < 0.05$) patients receiving antibiotic treatment. Error bars represent the SEM; * represents a significant difference.

Discussion

It has been proposed that a prolonged inflammatory response to foreign microorganisms promotes cancer, whereas certain commensal organisms reduce inflammation and prevent cancer development (30). *H. pylori* is a well-established cause of gastric adenocarcinoma and MALT lymphoma, but the hypothesis that *H. pylori* and/or other bacterial species contribute to a range of cancers is only beginning to gain traction. For example, *Helicobacter hepaticus*, which colonizes the intestine, has been shown to synergize with aflatoxin or hepatitis B virus to cause liver cancer in mice. In that model, β-catenin nuclear translocation was observed in tumors from animals exposed to both aflatoxin and *H. hepaticus*, but not in those treated with aflatoxin alone, thereby suggesting that both stimuli are involved in the cancer process (31). Other bacteria are also likely to influence cancer risk. *Salmonella typhi* is a known risk factor for gallbladder cancer, and several species, including *Propionibacterium acnes*, have been proposed as contributors to prostate cancer (32, 33). *Klebsiella pneumoniae* and *Proteus mirabilis* cause colon cancer in $Tbet^{-/-}$ and $Rag2^{-/-}$ ulcerative colitis (TRUC) mice through undetermined mechanisms (30). Furthermore, it is worth noting that MALT lymphoma and diffuse large B-cell lymphoma can often be treated solely by eradicating *H. pylori*, indicating that ongoing interactions with *H. pylori* are crucial for the survival of these tumors (34, 35).

Given this burgeoning role of bacteria in carcinogenesis and 2 previous reports that suggested that pseudomyxoma peritonei patients showed positive outcomes following antibiotic treatment (36, 37), we have investigated the molecular mechanisms by which bacteria may influence pseudomyxoma peritonei development. Importantly, our studies provide the first mechanistic data on the role of bacterial infection and β-catenin in pseudomyxoma peritonei. The data presented herein confirm our previous study that showed that bacterial density is higher in PMCA patients than in DPAM patients (23). If inflammation-inducing bacteria contribute to carcinogenesis, then one might posit that tumors with higher bacterial densities would be more malignant than those with fewer bacteria. Thus, our results are consistent with this hypothesis, because we found that the more aggressive PMCA tumors harbor more bacteria than the less aggressive DPAM tumors. Using a specific ISH method to identify bacteria, TNCB and *H. pylori* densities decreased significantly after antibiotic treatment in PMCA patients and to a lesser extent in DPAM patients. It is worth noting that a small number of bacteria remained alive following antibiotic treatment; thus, a different antimicrobial regimen, an extended treatment period, or the alteration of the timing or route of administration may be necessary to prevent regrowth of bacteria and possible stimulation of tumor growth. However, the antibiotic treatment used in this study clearly reduced the bacterial density within the tumors.

In contrast to the recent identification of the influence of bacterial species on cancer development, aberrant β-catenin localization and signaling is a well-established hallmark of carcinogenesis and metastasis. β-Catenin is a transmembrane protein that aids in cell-to-cell junctions, but it can also influence gene transcription within the nucleus. Translocation of β-catenin to the nucleus through its association with the Wnt signaling pathway is very important in embryogenesis and stem cell maintenance; however, it also contributes to abnormal proliferation during carcinogenesis. Indeed, the heterogeneous distribution of β-catenin within tumors suggests crosstalk between tumor cells and the tumor microenvironment, including epithelial–mesenchymal interaction and the vasculature (38). Moreover, in cancer, Wnt-β catenin-TCF signaling plays an important role in nuclear β-catenin accumulation (39), but the mechanisms governing this translocation are poorly understood and controversial (40).

Given the established role of β-catenin in carcinogenesis, it was pertinent to investigate the effect of antibiotic treatment and reduction in bacterial density on β-catenin expression and localization. Careful analysis of β-catenin expression and cellular distribution after antibiotic treatment targeted against *H. pylori* infection revealed important reductions in nuclear and total β-catenin levels in antibiotic-treated PMCA patients. The effects of antibiotic

treatment reached statistical significance primarily in PMCA samples and not in DPAM samples, which could be the result of the small sample size ($n = 6$) of antibiotic treated DPAM patients, making it more difficult to reach statistical significance; similar trends were seen in both groups of antibiotic-treated patients. The levels and localization of β-catenin were also altered throughout the various cell types within the analyzed peritoneal tissue, where antibiotic treatment significantly decreased β-catenin expression in the cytoplasm of epithelial and inflammatory cells, in the nuclei, and in the mucin of PMCA patients. Although not statistically significant, stromal β-catenin localization was elevated in PMCA patients not treated with antibiotics. Increased levels of β-catenin within the stroma is associated with desmoplastic reaction in malignancy (Fig. 4D), where β-catenin is attached to the fibrous elements of connective tissue of the stromal compartment (41). The stromal compartment plays an important role during neoplastic cell invasion, detaching from neoplastic intestinal glands, invading the stromal blood vessels and lymphatics, and initiating metastasis (42). β-Catenin within mucin was higher in PMCA patients as compared to DPAM patients. Unlike the stroma, antibiotic treatment had a significant effect on decreasing β-catenin in the mucin. Because mucin is the most important histopathology hallmark of pseudomyxoma peritonei, decreased levels of β-catenin within mucin after antibiotic treatment suggests that antimicrobials might be useful in the treatment of this disease. The effectiveness of antibiotic treatment is further evidenced by the significant elevation of β-catenin levels within the membrane in both PMCA and DPAM patients accompanied by a reduction in nuclear β-catenin levels following administration of antibiotics. In normal cells, the β-catenin complex is present within the adherens junctions, as confirmed by immunogold and transmission electron microscopy (43, 44). β-Catenin within the membrane promotes cell-to-cell communication and is likely to reduce neoplastic cell migration toward the stroma and metastasis; thus, increased levels of β-catenin within the membrane could be helpful in improving the prognosis of pseudomyxoma peritonei disease. Moreover, the renormalization of β-catenin distribution in PMCA patients after antibiotic treatment confirms the pivotal contribution of bacteria to the pseudomyxoma peritonei disease process.

Targeting nuclear β-catenin is a potential strategy for cancer therapy. Other reports have discussed the benefit of using antimicrobial agents to treat cancer; however, most attribute normalization of β-catenin with specific effects of antimicrobial agents on the Wnt/β-catenin pathway unrelated to the killing of microorganisms. For example, patients with ovarian endometric adenocarcinoma receiving rapamycin had a demonstrated inhibition of the Wnt/β-catenin pathway along with a decrease in tumor burden (45). Rapamycin blocks Wnt-mediated cell growth by interacting with mTOR, which is a central regulator of cell growth (46). Similarly, the antibiotic Streptonigrin was reported to block the complex formation of β-catenin/TCF (T-cell factor signaling) with DNA in human cell lines (47). In our study, the reduction of nuclear β-catenin following treatment with antimicrobial agents is likely due to bacterial killing, because, to our knowledge, no evidence indicates that amoxicillin or clarithromycin influence the Wnt/β-catenin signaling pathway. Of note, companion studies conducted by our group (J.J. Gilbreath et al., submitted for publication) have defined the microbiome of pseudomyxoma peritonei tumors from 11 patients and shown the ability to culture bacteria directly from pseudomyxoma peritonei tumor tissue. That study further indicated that antibiotic administration improves the survival of PMCA patients without pseudomyxoma peritonei observed in the lymph nodes when compared with untreated patients and historical data. Antibiotic treatment did not improve the survival of patients with lymph nodes positive for pseudomyxoma peritonei. Thus, treatment with antibiotics may be a beneficial therapy for pseudomyxoma peritonei patients with nonmetastatic disease.

We have not determined which mechanism is responsible for the reduction of nuclear β-catenin following antibiotic treatment or whether bacteria other than *H. pylori* contribute to abnormal β-catenin localization. It is plausible that the diminished β-catenin levels could be due to the loss of direct contact between tumor cells and bacteria or caused by a reduced inflammatory response to bacteria. In fact, DeNardo and colleagues propose that chronic inflammation could lead to Wnt/β-catenin activation without specific interactions between bacteria and epithelial cells (48). In this model, TNF-α produced by activated macrophages binds to TNF receptors on nearby epithelial cells, leading to AKT phosphorylation and the subsequent stabilization of β-catenin.

Recent studies have revealed the influence of several bacterial species on β-catenin expression and localization. *H. pylori* is present in the intercellular spaces, where the bacteria disrupt apical tight junctions as well as perturb molecular expression of β-catenin and other proteins of the lateral cell-to-cell membrane (49, 50). *Salmonella* activates the Wnt/β-catenin pathway via the secreted effector protein AvrA (21). *Campylobacter rodentium*, *Bacteroides fragilis*, and *Chlamydia trachomatis* also influence Wnt/β-catenin signaling (15, 22). Given the effect of bacteria on β-catenin signaling, which is known to contribute to the carcinogenic process, it is interesting to note that many common cancers occur in anatomical regions frequently exposed to bacteria, including cancers of the throat, lung, gastrointestinal tract, reproductive tract, and skin. Other locations, such as the breast, may seem to exist as sterile sites; however, bacteria can often gain entry, raising the possibility that individual bacterial species or a combination of different species could contribute to the carcinogenic process in multiple cancers. Thus, determining which bacterial species are involved in these processes could lead to targeted antimicrobial therapy and help to improve current methods for preventing and treating cancer.

Disclosure of Potential Conflicts of Interest

No potential conflicts of interest were disclosed.

Authors' Contributions

Conception and design: C. Semino-Mora, T.L. Testerman, C. Nieroda, D.S. Merrell, A. Dubois

Development of methodology: C. Semino-Mora, T.J. McAvoy, C. Nieroda

Acquisition of data (provided animals, acquired and managed patients, provided facilities, etc.): C. Semino-Mora, H. Liu, K. Studeman, Y. Jia, C. Nieroda

Analysis and interpretation of data (e.g., statistical analysis, biostatistics, computational analysis): C. Semino-Mora, T.L. Testerman, H. Liu, T.J. McAvoy, D.S. Merrell, A. Dubois

Writing, review, and/or revision of the manuscript: C. Semino-Mora, T.L. Testerman, J.M. Whitmire, T.J. McAvoy, C. Nieroda, A. Sardi, D.S. Merrell, A. Dubois

Administrative, technical, or material support (i.e., reporting or organizing data, constructing databases): H. Liu, T.J. McAvoy, J. Francis

Study supervision: A. Sardi, D.S. Merrell, A. Dubois

Acknowledgments

During the writing of this article, Dr. A. Dubois passed away unexpectedly. Although ill for a length of time, he did not want others to be concerned and was silent about this fact. Throughout his illness, he worked diligently and passionately on the pseudomyxoma peritonei research. His wisdom, generosity, and expertise will be sorely missed by his colleagues and the research community. In addition, Dr. C. Semino-Mora passed away after the submission of the original manuscript. Despite a lengthy illness, she continued to contribute her abilities to several research projects. Her extensive skills and expertise were a tremendous asset that cannot be replaced. The authors thank Dr. D. McDaniel for his assistance with laser confocal imaging along with M. Sittig and M. Putman for their contributions to this project.

Grant Support

This work was supported by R0832L, which was funded by Uniformed Services University, as well as funding from the US Military Cancer Institute. The study was approved by the Institutional Review Boards of the Mercy Medical Center and the Uniformed Services University of the Health Sciences, and written informed consent was obtained from all patients before study entry.

The costs of publication of this article were defrayed in part by the payment of page charges. This article must therefore be hereby marked *advertisement* in accordance with 18 U.S.C. Section 1734 solely to indicate this fact.

Received March 7, 2013; revised May 10, 2013; accepted May 27, 2013; published OnlineFirst June 6, 2013.

References

1. Bradley RF, Stewart JHt, Russell GB, Levine EA, Geisinger KR. Pseudomyxoma peritonei of appendiceal origin: a clinicopathologic analysis of 101 patients uniformly treated at a single institution, with literature review. Am J Surg Pathol 2006;30:551–9.
2. Mann WJ Jr, Wagner J, Chumas J, Chalas E. The management of pseudomyxoma peritonei. Cancer 1990;66:1636–40.
3. Aho AJ, Heinonen R, Lauren P. Benign and malignant mucocele of the appendix. Histological types and prognosis. Acta Chir Scand 1973;139:392–400.
4. Smeenk RM, Bruin SC, van Velthuysen ML, Verwaal VJ. Pseudomyxoma peritonei. Curr Probl Surg 2008;45:527–75.
5. Witkamp AJ, de Bree E, Van Goethem R, Zoetmulder FA. Rationale and techniques of intra-operative hyperthermic intraperitoneal chemotherapy. Cancer Treat Rev 2001;27:365–74.
6. Galani E, Marx GM, Steer CB, Culora G, Harper PG. Pseudomyxoma peritonei: the 'controversial' disease. Int J Gynecol Cancer 2003;13:413–8.
7. Loungnarath R, Causeret S, Brigand C, Gilly FN, Glehen O. [Pseudomyxoma peritonei: new concept and new therapeutic approach]. Ann Chir 2005;130:63–9.
8. Levine EA, Stewart JHt, Russell GB, Geisinger KR, Loggie BL, Shen P. Cytoreductive surgery and intraperitoneal hyperthermic chemotherapy for peritoneal surface malignancy: experience with 501 procedures. J Am Coll Surg 2007;204:943–53; discussion 53-5.
9. Gough DB, Donohue JH, Schutt AJ, Gonchoroff N, Goellner JR, Wilson TO, et al. Pseudomyxoma peritonei. Long-term patient survival with an aggressive regional approach. Ann Surg 1994;219:112–9.
10. Halabi HE, Gushchin V, Francis J, Athas N, Macdonald R, Nieroda C, et al. Prognostic significance of lymph node metastases in patients with high-grade appendiceal cancer. Ann Surg Oncol 2012;19:122–5.
11. Yan H, Pestieau SR, Shmookler BM, Sugarbaker PH. Histopathologic analysis in 46 patients with pseudomyxoma peritonei syndrome: failure versus success with a second-look operation. Mod Pathol 2001;14:164–71.
12. Miller JR. The Wnts. Genome Biol 2001;3:REVIEWS3001-REVIEWS3001.15.
13. Hayashida Y, Honda K, Idogawa M, Ino Y, Ono M, Tsuchida A, et al. E-cadherin regulates the association between beta-catenin and actinin-4. Cancer Res 2005;65:8836–45.
14. Takayama T, Shiozaki H, Shibamoto S, Oka H, Kimura Y, Tamura S, et al. Beta-catenin expression in human cancers. Am J Pathol 1996;148:39–46.
15. Sun J. Enteric bacteria and cancer stem cells. Cancers (Basel) 2010;3:285–97.
16. Hayward SD, Liu J, Fujimuro M. Notch and Wnt signaling: mimicry and manipulation by gamma herpesviruses. Sci STKE 2006;2006:re4.
17. Zhang Y, Wei W, Cheng N, Wang K, Li B, Jiang X, et al. Hepatitis C Virus-induced upregulation of miR-155 promotes hepatocarcinogenesis by activating Wnt signaling. Hepatology 2012;56:1631–40.
18. El-Etr SH, Mueller A, Tompkins LS, Falkow S, Merrell DS. Phosphorylation-independent effects of CagA during interaction between *Helicobacter pylori* and T84 polarized monolayers. J Infect Dis 2004;190:1516–23.
19. Franco AT, Israel DA, Washington MK, Krishna U, Fox JG, Rogers AB, et al. Activation of beta-catenin by carcinogenic *Helicobacter pylori*. Proc Natl Acad Sci U S A 2005;102:10646–51.
20. Nakopoulou L, Mylona E, Papadaki I, Kavantzas N, Giannopoulou I, Markaki S, et al. Study of phospho-beta-catenin subcellular distribution in invasive breast carcinomas in relation to their phenotype and the clinical outcome. Mod Pathol 2006;19:556–63.
21. Liu X, Lu R, Wu S, Sun J. *Salmonella* regulation of intestinal stem cells through the Wnt/beta-catenin pathway. FEBS Lett 2010;584:911–6.
22. Kessler M, Zielecki J, Thieck O, Mollenkopf HJ, Fotopoulou C, Meyer TF. *Chlamydia trachomatis* disturbs epithelial tissue homeostasis in fallopian tubes via paracrine Wnt signaling. Am J Pathol 2012;180:186–98.
23. Semino-Mora C, Liu H, McAvoy T, Nieroda C, Studeman K, Sardi A, et al. Pseudomyxoma peritonei: is disease progression related to microbial agents? A study of bacteria, MUC2 AND MUC5AC expression in disseminated peritoneal adenomucinosis and peritoneal mucinous carcinomatosis. Ann Surg Oncol 2008;15:1414–23.
24. Ronnett BM, Zahn CM, Kurman RJ, Kass ME, Sugarbaker PH, Shmookler BM. Disseminated peritoneal adenomucinosis and peritoneal mucinous carcinomatosis. A clinicopathologic analysis of 109 cases with emphasis on distinguishing pathologic features, site of origin, prognosis, and relationship to "pseudomyxoma peritonei." Am J Surg Pathol 1995;19:1390–408.
25. Liu H, Merrell DS, Semino-Mora C, Goldman M, Rahman A, Mog S, et al. Diet synergistically affects *Helicobacter pylori*-induced gastric carcinogenesis in nonhuman primates. Gastroenterology 2009;137:1367–79 e1–6.
26. Liu H, Rahman A, Semino-Mora C, Doi SQ, Dubois A. Specific and sensitive detection of *H. pylori* in biological specimens by real-time RT-PCR and *in situ* hybridization. PLoS One 2008;3:e2689.
27. Semino-Mora C, Doi SQ, Marty A, Simko V, Carlstedt I, Dubois A. Intracellular and interstitial expression of *Helicobacter pylori* virulence

genes in gastric precancerous intestinal metaplasia and adenocarcinoma. J Infect Dis 2003;187:1165–77.
28. Lan ZD, Dai L, Zhuo XL, Feng JC, Xu K, Chi CW. Gene cloning and sequencing of BmK AS and BmK AS-1, two novel neurotoxins from the scorpion *Buthus martensi* Karsch. Toxicon 1999;37:815–23.
29. Dixon MF, Genta RM, Yardley JH, Correa P. Histological classification of gastritis and *Helicobacter pylori* infection: an agreement at last? The International Workshop on the Histopathology of Gastritis. Helicobacter 1997;2 Suppl 1: S17–24.
30. Trinchieri G. Cancer and inflammation: an old intuition with rapidly evolving new concepts. Annu Rev Immunol 2012;30:677–706.
31. Martin HR, Shakya KP, Muthupalani S, Ge Z, Klei TR, Whary MT, et al. *Brugia filariasis* differentially modulates persistent *Helicobacter pylori* gastritis in the gerbil model. Microbes Infect 2010;12:748–58.
32. Samaras V, Rafailidis PI, Mourtzoukou EG, Peppas G, Falagas ME. Chronic bacterial and parasitic infections and cancer: a review. J Infect Dev Ctries 2010;4:267–81.
33. Fassi Fehri L, Mak TN, Laube B, Brinkmann V, Ogilvie LA, Mollenkopf H, et al. Prevalence of *Propionibacterium acnes* in diseased prostates and its inflammatory and transforming activity on prostate epithelial cells. Int J Med Microbiol 2011;301:69–78.
34. Kuo SH, Yeh KH, Wu MS, Lin CW, Hsu PN, Wang HP, et al. *Helicobacter pylori* eradication therapy is effective in the treatment of early-stage *H. pylori*-positive gastric diffuse large B-cell lymphomas. Blood 2012;119:4838–44; quiz 5057.
35. Ferreri AJ, Govi S, Raderer M, Mule A, Andriani A, Caracciolo D, et al. *Helicobacter pylori* eradication as exclusive treatment for limited-stage gastric diffuse large B-cell lymphoma: results of a multicenter phase 2 trial. Blood 2012;120:3858–60.
36. Creel NJ, Dart BWt. Goblet cell carcinoid and mucinous cystadenoma in an interval appendectomy specimen. Am Surg 2012;78:E49–50.
37. Thompson MA, Ashton RW, Pitot HC. Mucinous appendiceal adenocarcinoma presenting 5 years after appendectomy. Ann Intern Med 2004;140:W33.
38. Fisher M, Huang YS, Li X, McIver KS, Toukoki C, Eichenbaum Z. Shr is a broad-spectrum surface receptor that contributes to adherence and virulence in group A streptococcus. Infect Immun 2008;76:5006–15.
39. van de Wetering M, Sancho E, Verweij C, de Lau W, Oving I, Hurlstone A, et al. The beta-catenin/TCF-4 complex imposes a crypt progenitor phenotype on colorectal cancer cells. Cell 2002; 111:241–50.
40. Wu X, Tu X, Joeng KS, Hilton MJ, Williams DA, Long F. Rac1 activation controls nuclear localization of beta-catenin during canonical Wnt signaling. Cell 2008;133:340–53.
41. Osunkoya AO, Netto GJ, Epstein JI. Colorectal adenocarcinoma involving the prostate: report of 9 cases. Hum Pathol 2007;38: 1836–41.
42. Karagiannis GS, Petraki C, Prassas I, Saraon P, Musrap N, Dimitromanolakis A, et al. Proteomic signatures of the desmoplastic invasion front reveal collagen type XII as a marker of myofibroblastic differentiation during colorectal cancer metastasis. Oncotarget 2012;3: 267–85.
43. Aberle H, Schwartz H, Kemler R. Cadherin-catenin complex: protein interactions and their implications for cadherin function. J Cell Biochem 1996;61:514–23.
44. Bierkamp C, Schwarz H, Huber O, Kemler R. Desmosomal localization of beta-catenin in the skin of plakoglobin null-mutant mice. Development 1999;126:371–81.
45. Tanwar PS, Zhang L, Kaneko-Tarui T, Curley MD, Taketo MM, Rani P, et al. Mammalian target of rapamycin is a therapeutic target for murine ovarian endometrioid adenocarcinomas with dysregulated Wnt/beta-catenin and PTEN. PLoS One 2011;6:e20715.
46. Inoki K, Ouyang H, Zhu T, Lindvall C, Wang Y, Zhang X, et al. TSC2 integrates Wnt and energy signals via a coordinated phosphorylation by AMPK and GSK3 to regulate cell growth. Cell 2006;126:955–68.
47. Park S, Chun S. Streptonigrin inhibits beta-catenin/Tcf signaling and shows cytotoxicity in beta-catenin-activated cells. Biochim Biophys Acta 2011;1810:1340–5.
48. DeNardo DG, Johansson M, Coussens LM. Inflaming gastrointestinal oncogenic programming. Cancer Cell 2008;14:7–9.
49. Necchi V, Candusso ME, Tava F, Luinetti O, Ventura U, Fiocca R, et al. Intracellular, intercellular, and stromal invasion of gastric mucosa, preneoplastic lesions, and cancer by *Helicobacter pylori*. Gastroenterology 2007;132:1009–23.
50. Suzuki M, Mimuro H, Suzuki T, Park M, Yamamoto T, Sasakawa C. Interaction of CagA with Crk plays an important role in *Helicobacter pylori*-induced loss of gastric epithelial cell adhesion. J Exp Med 2005; 202:1235–47.